ACS APPLIED ENGINEERING MATERIALS

pubs.acs.org/acsaenm Article

Unveiling the Potential of $[Sn_2S_6]^{4-}$ Functionalized Layered Double Hydroxides for the Sorption of ReO_4^- as a Surrogate for $^{99}TcO_4^-$

Ahmet Celik, Subrata Chandra Roy, Michael A. Quintero, Kathryn Taylor-Pashow, Dien Li, Mercouri G. Kanatzidis, Xianchun Zhu, and Saiful M. Islam*

Cite This: https://doi.org/10.1021/acsaenm.3c00074 Read Online

ACCESS | Metrics & More | Article Recommendations | Supporting Information

ABSTRACT: Technetium (^{99}Tc) is a long-live radionuclide, and its removal from legacy nuclear waste is problematic mainly because of its persistence as highly soluble pertechnetate ($^{99}TcO_4^-$) ions. Here, we report the application of $[Sn_2S_6]^{4-}$ anion intercalated layered double hydroxides, LDH-$[Sn_2S_6]$ for the removal of perrhenate (ReO_4^-), a nonradioactive surrogate of $^{99}TcO_4^-$. In acidic and neutral media, LDH-$[Sn_2S_6]$ can remove over 98 and 96% of ReO_4^-, respectively, from a 1000 ppb spiked solution in 48 h, and the removal of ReO_4^- remains beyond 87% even after 15 days of interaction with the solution. Moreover, in the presence of other metal ions, for instance, Cu^{2+}, ReO_4^- removal increases to about 99.9%, leaving the residual concentration of <1 ppb with $K_d \sim 5.00 \times 10^7$ mL/g. LDH-$[Sn_2S_6]$ also exhibits large sorption capacities for ReO_4^- at 9.3×10^4 μg/g at pH ~ 2. Evidenced by XRD, SEM, HRTEM, EDS, and XPS, we further demonstrate the removal of ReO_4^- occurs by ion-exchange and precipitation. Overall, the roles of 3d transition metal ions and the pH-driven sorption mechanisms introduce remarkable insights into metal sulfides intercalated LDH to remove $^{99}TcO_4^-$.

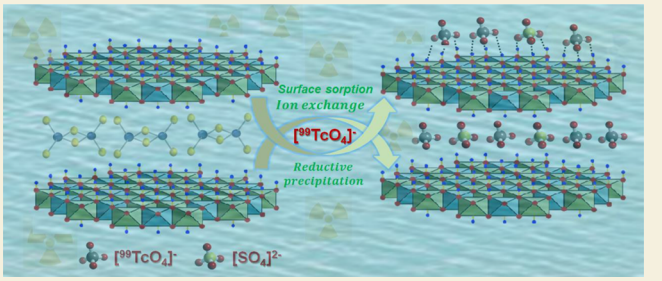

KEYWORDS: *nuclear waste, pertechnetate, perrhenate, LDH-$[Sn_2S_6]$, technetium*

1. INTRODUCTION

Technetium-99 (^{99}Tc) is produced through high-yield fission of uranium (^{235}U), which embraces a very long half-life ($t_{1/2}$ = 2.13 × 10^5 years).[1−4] Additionally, ^{99}Tc is highly soluble in water (11.3 mol/L at 20 °C) where it exists as $^{99}TcO_4^-$ anion and possesses a noncomplexing nature.[2,3,5] These result in high mobility in the surface and terrestrial environment; thus, it poses severe risks to biological systems, including humans.[6−9] The release of ^{99}Tc from Hanford sites has caused contamination in groundwater which is at least 10 times higher than the highest contaminant level set by the US EPA (900 pCi/L).[10] Therefore, it is important to remove $^{99}TcO_4^-$ from defense legacy nuclear waste and contaminated water.

The removal of ^{99}Tc from nuclear waste has been accomplished using various methods and materials, but each has shortcomings. For instance, Purolite A520E is an ion exchange resin that shows an efficient uptake of TcO_4^- from simulated nuclear wastewater, but it exhibits poor irradiation stability and has sluggish anion-exchange kinetics.[9] In recent years, metal−organic frameworks (MOFs), specifically cationic MOFs, have appealed to attention because of their efficient uptake of TcO_4^- from defense legacy nuclear waste, but their complex synthetic procedures, scalability, reusability, and high cost hinder their practical application.[11−13] On the other hand, layered double hydroxides (LDHs), a hydrotalcite type clay, are attractive because of their low cost, scalability, and efficient sorption properties for TcO_4^-. LDH can be defined by the general formula $[M^{II}_{(1-x)}M^{III}_x\ (OH)_2]^{x+}[(A^{n-})_{x/n}{\cdot}mH_2O]^{x-}$, where M^{II} and M^{III} correspond to divalent and trivalent cations and A^{n-} is an anion.[14−18] In LDH, the positively charged metal hydroxide layers are counterbalanced with exchangeable anions that inhabit the interlayer spacings.[14,15] Because of such distinct structural features, LDHs adopt diverse sorption mechanisms for TcO_4^- and its oxoanionic surrogates, such as adsorption on the outer surface via M^{2+}/M^{3+}−O−H···O_4−Tc interactions, ion-exchange-driven trapping in between the positively charged host LDH layers, and reconstruction of the LDH structures.[6] Furthermore, metal sulfides/polysulfides are known to remove TcO_4^- from the solution by reductive precipitation ($Tc^{7+}_{(sol)} \rightarrow Tc^{4+}_{(s)}$) and surface sorption through S···TcO_4 covalent interactions.[19−22] These features, along with the LDH's intrinsic sorption properties toward TcO_4^-, appealed to us to design and fabricate an LDH with metal sulfide anions to produce LDH-Mo_3S_{13}.[16] It should be noted that structurally $Mo_3S_{13}^{2-}$ is presented as $[Mo^{IV}_3S(S_2)_6]^{2-}$,

Received: February 23, 2023
Revised: June 21, 2023
Accepted: June 21, 2023

where the trinuclear cluster of Mo^{4+} ions are surrounded by six disulfide (S_2^{2-}) groups and an epical S^{2-} anion.[23] Our investigations demonstrated that the removal of CrO_4^{2-}, a redox surrogate of TcO_4^-, occurs mainly through reductive precipitation where cooperative oxidation of S_2^{2-} and Mo^{4+} infers the reductive precipitation of soluble Cr^{6+} to insoluble Cr^{3+}.[16] This intriguing finding requires further investigation of diverse metal sulfide anion intercalated LDHs and analysis of their sorption mechanisms under different experimental conditions.

In this study, we present a new sorbent called LDH-$[Sn_2S_6]$, which is intercalated with $[Sn_2S_6]^{4-}$, for removing ReO_4^-, a nonradioactive surrogate for $^{99}TcO_4^-$, from aqueous solutions. We demonstrate that LDH-$[Sn_2S_6]$ is able to effectively remove ReO_4^- from both acidic and neutral solutions, and its effectiveness is further improved in the presence of a transition metal cation. We also show the removal of ReO_4^- occurs through ion exchange and precipitation. This finding reveals important insights into the sorption mechanisms of metal-intercalated LDHs for ReO_4^-, a representative $^{99}TcO_4^-$.

2. EXPERIMENTAL SECTION

2.1. Synthesis of LDH-$[Sn_2S_6]$

Stannic sulfide $[Sn_2S_6]^{4-}$-intercalated magnesium aluminum LDHs, MgAl-$[Sn_2S_6]$ (LDH-$[Sn_2S_6]$) were synthesized from MgAl–NO_3 (LDH-NO_3) by the exchange of nitrate anion with $[Sn_2S_6]^{4-}$ following a procedure described previously.[24] Specifically, for the synthesis of LDH-$[Sn_2S_6]$, the ion exchange was conducted by stirring the suspension of 0.05 g LDH-NO_3 and 0.15 g $Na_4Sn_2S_6{\cdot}14H_2O$ in 10 mL deionized water (DIW) for 24 h under ambient conditions.[24] The pale yellow solids were recovered after filtration, ethanol washing, and drying under room ambient conditions. White crystals of $Na_4Sn_2S_6{\cdot}14H_2O$ were synthesized from a solution of 14.4 g (59.96 mmol) $Na_2S{\cdot}9H_2O$ and 5.2 g (14.8 mmol) $SnCl_4{\cdot}5H_2O$ in the refrigerator according to the literature.[25] Beforehand, LDH-NO_3 was synthesized following the steps specified in the literature.[16,24]

2.2. Sorption Experiments

The uptake experiment of aqueous ReO_4^- (1×10^3–3×10^5 ppb) was performed by the batch method at room temperature. After mixing the solid sorbent of LDH-$[Sn_2S_6]$ (10.0 mg) with the aqueous ReO_4^- solutions (10.0 mL) for a certain time, the supernatant solutions were separated from solid sorbents by centrifugation. The adsorption experiments were performed with the $V{:}m$ ratio of 1000 mL/g, at room temperature and at different times ranging from minutes to days. Subsequently, the supernatants were analyzed by inductively coupled plasma-mass spectrometry (ICP-MS). Characterizations of the solid adsorbent after sorption experiments were performed by X-ray diffraction (XRD), energy dispersive spectroscopy (EDS), and X-ray photoelectron spectroscopy (XPS).

The distribution coefficient (K_d) in sorption experiments was used as a tool to determine the affinity of LDH-Sn_2S_6 for ReO_4^-. The distribution coefficient, K_d (mL/g), removal (%), and sorption capacity q_m (μg/g) are expressed by eqs 1–3, respectively.[26]

$$\text{Distribution coefficient: } K_d = \frac{\left(\frac{C_0 - C_e}{C_e}\right) \times V}{m} \quad (1)$$

$$\text{Removal percentage: } \frac{C_0 - C_e}{C_0} \times 100 \quad (2)$$

$$\text{Sorption capacity: } q_m = \frac{(C_0 - C_e) \times V}{m} \times 10^{-3} \quad (3)$$

where "V" is the volume of solution (mL), C_0 and C_e correspond to the initial and the final concentrations of the $[ReO_4]^-$ in ppb, and "m" is the mass of the solid sorbent (g).

2.3. Characterization

2.3.1. X-ray Powder Diffraction. XRD of the finely ground powder of the pristine and postinteracted LDH-$[Sn_2S_6]$ was collected on a Rigaku MiniFlex 600 diffractometer using Cu $K_{\alpha 1}$ (λ = 1.540593 Å) radiation, generated from a sealed-tube X-ray source at 40 kV and 15 mA equipped with a D/teX Ultra detector. The intensity data from the diffraction experiments were collected at a scan rate of 5° min^{-1} (0.02° resolution).

2.3.2. Electron Microscopy Imaging and EDS. A Lyra3-Tescan scanning electron microscope (SEM) was used for elemental analysis and imaging of the samples. An accelerating voltage of 20 kV and about 120 s of accumulation time were retained throughout data collection time. Elemental analysis was performed using the Environmental Secondary Electron Detector (ESED-II). The powdered samples were placed on a carbon-taped metal stub for imaging of the surface morphology and quantitative determinations of the elemental compositions of the samples. EDS analysis was performed at least four different spots and the average was used to identify the compositions.

2.3.3. Transmission Electron Microscopy. Thermofisher Talos F200X was used to analyze at an accelerating voltage of 200 kV. The imaging was done in transmission electron microscopy (TEM) mode. The samples were dispersed in ethanol and were drop cast on a TEM carbon grid.

2.3.4. Inductively Coupled Plasma-Mass Spectrometry. Inductively coupled plasma-mass spectrometry (ICP-MS) was performed to determine the metal ion concentrations in the supernatant solutions after sorption using a Varian ICP-MS instrument (model: 820-MS). The detection limit of Re in the water sample is below 1 ppb. Analytical quality control was verified and maintained after every 10 samples with a QC/QA sample prepared from certified single-element reference material purchased from Spex CertiPrep (certified by DQS to ISO 9001:2015 and accredited by A2LA to ISO/IEC 17025:2017 and ISO 17034:2016).

2.3.5. X-ray Photoelectron Spectroscopy. XPS spectra of the as-obtained samples were collected using an ESCALAB 250Xi spectrometer (Thermo Fisher) with Al-K_α X-ray as the radiation source, 500 μm spot size, and an electron flood gun to reduce sample charging. Before each spectra collection, the sample was etched with Ar at 30 KeV for 30 s for the surface cleanup. Each sample was measured in triplicate and all spectra have been charged shift corrected to the C1s peak at 284.8 eV.

3. RESULTS AND DISCUSSION

LDH-$[Sn_2S_6]$ nanosheets were synthesized by the exchange of the NO_3^- anions of the LDH-NO_3 with the $[Sn_2S_6]^{4-}$ anions at room temperature, as described previously.[24] The synthesis of the LDH-$[Sn_2S_6]$ has been confirmed using EDS, XPS, and XRD. The EDS and XPS showed the presence of Sn and S in addition to Mg and Al; while XRD showed an increase in the d-spacing of the basal reflection, d_{003}, from the LDH-NO_3 (0.91 nm) to LDH-$[Sn_2S_6]$ (1.08 nm) which is consistent with the larger size of the $[Sn_2S_6]$ anions.[24]

We investigated the sorption properties of LDH-$[Sn_2S_6]$ for ReO_4^- as a nonradioactive surrogate of $^{99}TcO_4^-$ by batch sorption experiments at various times, concentrations, pHs, and the presence of cations and anions. The sorption experiments that we performed for a 1000 ppb of Re^{7+} (as ReO_4^-) spiked solution showed that LDH-$[Sn_2S_6]$ could remove about 47, 78, and 96% of ReO_4^- in 1, 24, and 96 h, respectively, at pH ~ 7 (Figure 1 and Table S1). This led to the distribution constant, K_d being as high as $\sim \geq 10^4$ mL/g. Notably, K_d values with an order of magnitude $\sim 10^4$ mL/g suggest a high affinity of a sorbent to a sorbate.[26] This indicates that LDH-$[Sn_2S_6]$ is an effective sorbent for ReO_4^- ions. In contrast, in the acidic solutions of pH ~ 2, LDH-$[Sn_2S_6]$ can remove about 49% Re^{7+} in 1 h, while it reaches over 95 and

https://doi.org/10.1021/acsaenm.3c00074
ACS Appl. Eng. Mater. XXXX, XXX, XXX–XXX

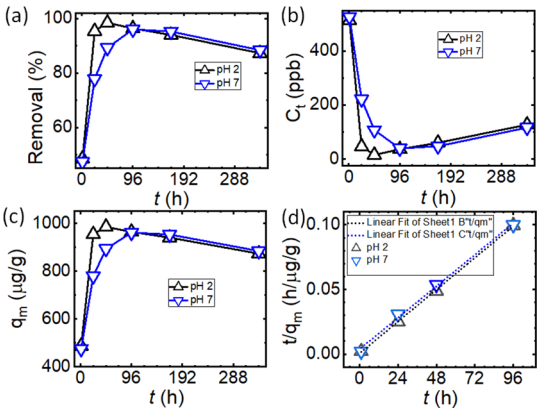

Figure 1. Time-dependent sorption experiments of Re^{7+} for LDH-Sn_2S_6 as ReO_4^- at neutral (pH ~ 7) and acidic (pH ~ 2) media showing (a) removal percentage, (b) change of Re^{7+} ion concentration, (c) sorption capacity, and (d) pseudo-second-order adsorption rate.

98% in 24 and 48 h, respectively (Figure 1 and Table S1). These led to residual concentrations of rhenium ions as low as 15 ppb. Remarkably, our findings reveal that Re^{7+} removal efficiencies remain over 87% even after 15 days of interactions of ReO_4^- with LDH-Sn_2S_6 in acidic and neutral solutions. Hence, the slow decomposition of the LDH structure over an extended period may be attributed to the release of rhenium in the solution. Despite this, the removal reaches a maximum in 3 days of interactions which may suggest that LDH-$[Sn_2S_6]$ is resilient against decompositions in acidic and neutral solutions in this time scale and effectively stores rhenium ions in the solid matrixes. Apart from this, a partial reoxidation of the insoluble Re^{4+} species to the soluble Re^{7+} cannot be ruled out.[27]

To understand the sorption behavior of LDH-$[Sn_2S_6]$ for ReO_4^-, we utilized pseudo-first-order and pseudo-second-order rate equations as expressed in eqs 4 and 5.[28] Following these rate equations, we investigated the sorption mechanisms of LDH-$[Sn_2S_6]$ for ReO_4^- to demonstrate the kinetics data, and then we compared the experimental and calculated data.

$$\text{Pseudo} - \text{first order: } \ln(q_e - q_t) = \ln q_e - k_1 t \quad (4)$$

$$\text{Pseudo} - \text{second order: } \frac{t}{q_t} = \frac{1}{k_2 q_e^2} + \frac{t}{q_e} \quad (5)$$

where q_e (μg/g) expresses the amount of adsorbed element per unit mass of adsorbent at equilibrium and q_t (μg/g) refers to the adsorbed amount at time t, while k_1 (min^{-1}) and k_2 (g/μg min^{-1}) express equilibrium rate constants of pseudo-first-order and pseudo-second-order adsorption interactions, respectively.[29] The k_1 value was acquired by plotting $\ln(q_e - q_t)$ against t and k_2 by plotting t/q_t against t.

We investigated the ReO_4^- removal kinetics by LDH-$[Sn_2S_6]$ for 1000 ppb of Re^{7+} (as ReO_4^-) spiked solutions at pH ~ 2 and ~7. Analysis of the kinetic data showed that the sorption of ReO_4^- followed the pseudo-second-order rate equation, and the rate constants obtained as 2.1×10^{-3} g·μg^{-1}·h^{-1} at pH ~ 2 and 2.7×10^{-4} g·μg^{-1}·h^{-1} at pH ~ 7 (Table S2). Figure 1d demonstrates a linear relationship derived from the plot of t/q_t vs t for both pH values (R^2 ~ 0.9997 and 0.9966, respectively). The rate constant at pH ~ 2 is roughly an order of magnitude higher than at pH ~ 7. This indicates that at pH ~ 2, LDH-$[Sn_2S_6]$ shows a superior ReO_4^- removal efficiency than at pH ~ 7. This finding corroborates the previous reports that showed an increase of ReO_4^- (as $^{99}TcO_4^-$ surrogate) removal efficiencies with the decrease of pH.[30−34] In addition, the distinction of the rate constants, 2.1×10^{-3} and 2.7×10^{-4} g·μg^{-1}·h^{-1} at these two pH values may indicate diverse ReO_4^- sorption mechanisms. Notably, an acceleration of removal efficiencies of ReO_4^- in acidic media can be attributed to the protonation of the surface of the 2D layers of the LDH. Hence, the oxides layers of the protonated LDH bind ReO_4^- through $M^{2+}/M^{3+}-O-H\cdots O_4-Re$ hydrogen bonding, as suggested previously for LDHs.[19,31,35−37]

To understand the impact on the sorption efficiencies in the presence of other transition metal cations, we introduced copper-II (Cu^{2+}) ion, as an example, along with $[ReO_4]^-$ spiked solutions. According to this study, the presence of Cu^{2+} ions significantly enhanced the removal of $[ReO_4]^-$. More specifically, with the addition of 1.0×10^4 ppb of Cu^{2+} ions in the 1.0×10^3 ppb spiked solutions of $[ReO_4]^-$, Re^{7+} removal increases to about 99.9% leaving the residual concentration below 1 ppb at pH ~ 2. This high removal led to a large value of distribution constant, K_d ~ 5.00×10^7 mL/g (Table 1). This

Table 1. Influence of the Sorption of ReO_4^- by LDH-$[Sn_2S_6]$ in the Presence of Cu^{2+} at Different pH and Concentrations[a]

	C_0 (ppb)			Re^{7+} removal		
pH	Re	Cu	C_t (ppb)	(%)	K_d (mL/g)	q_m (μg/g)
2	1×10^3		15.6	98.44	6.31×10^4	985
	1×10^3	1×10^4	0.02	99.99	5.00×10^7	999
	1×10^4		3026	69.74	2.30×10^3	6974
	1×10^4	1×10^4	3464	65.36	1.89×10^3	6536
7	1×10^3		107	89.31	8.34×10^3	893
	1×10^3	1×10^4	68	93.24	1.38×10^4	932
	1×10^4		9260	7.40	0.79×10^2	740
	1×10^4	1×10^4	6460	35.24	5.48×10^2	3540

[a]Contact time: 48 h; m: 10 mg; V: 10 mL; V/m: 10/0.01 = 1000 mL/g.

value of K_d is substantially higher than the values reported for the layer hydroxide salt, NiFe-LHS (3×10^3 mL/g),[38] LDH-CO_3 (4×10^2 mL/g), and calcined LDH-CO_3 (7×10^3 mL/g).[39] Similarly, at neutral pH, the removal efficiency increases from 89 to 93% upon the addition of 1.0×10^4 ppb of Cu^{2+} solution (Table 1). This kind of enhancement for the removal rate of other oxoanions was observed for LDH-MoS_4 in the presence of Hg^{2+}, Cu^{2+}, and Cd^{2+}.[40] This finding suggests that the addition of similar metals could enhance the removal rate of ReO_4^- for the LDH-Sn_2S_6.[40] Hence, the boost of the removal rate of ReO_4^- could be due to the formation of the larger $\{Cu_n[Sn_2S_6]\}^{4-n}$, where $n < 2$ for Cu^{2+} ions, anionic adducts which increases the interlayer distance of the LDH layers and thus facilitates the exchange of the smaller $[ReO_4]^-$ anions into LDH host. Apart from this, the precipitation of $\{Cu_2[Sn_2S_6]\}$ as noncrystalline neutral chemical species cannot be completely ruled out. However, the exact mechanism is not yet clearly understood. This is mainly because of the lack of available tools to analyze the chemical interactions during the interactions within the solutions.

Moreover, to determine the maximum sorption capacity of LDH-$[Sn_2S_6]$ for the removal of rhenium as $[ReO_4]^-$, we

https://doi.org/10.1021/acsaenm.3c00074
ACS Appl. Eng. Mater. XXXX, XXX, XXX−XXX

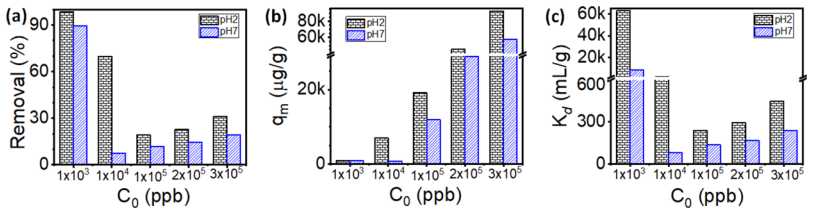

Figure 2. Concentration-dependent sorption of [ReO_4] by LDH-[Sn_2S_6] shows (a) removal percentage, (b) sorption capacity, and (c) distribution coefficient, K_d under neutral pH and ambient conditions.

Table 2. Concentration-Dependent Sorption of Re^{7+} by the LDH-[Sn_2S_6] at Different pH[a]

	C_t (ppb)		Re^{7+} removal (%)		K_d (mL/g)		q_m (μg/g)	
C_i (ppb)	pH 2	pH 7	pH 2	pH 7	pH 2	pH 7	pH 2	pH 7
1×10^3	0.02×10^3	0.10×10^3	98.4	89.2	631.0×10^2	82.9×10^2	9.84×10^2	8.93×10^2
1×10^4	0.30×10^4	0.93×10^4	69.7	7.4	23.0×10^2	0.79×10^2	6.97×10^3	7.40×10^2
1×10^5	0.80×10^5	0.88×10^5	19.3	11.9	2.39×10^2	1.36×10^2	1.93×10^4	1.19×10^4
2×10^5	1.54×10^5	1.71×10^5	22.7	14.4	2.94×10^2	1.69×10^2	4.54×10^4	2.89×10^4
3×10^5	2.07×10^5	2.42×10^5	30.9	19.2	4.48×10^2	2.38×10^2	9.28×10^4	5.77×10^4

[a]Contact time: 48 h; m: 10 mg; V: 10 mL; V/m: 10/0.01 = 1000 mL/g.

investigated its removal efficiencies at various starting concentrations, ranging from 1×10^3 to 3×10^5 ppb. The maximum sorption capacity of LDH-[Sn_2S_6] for rhenium was determined by using the adsorption equilibrium at pH ~ 2 and ~7 (Figure 2b and Table 2). This investigation revealed that LDH-[Sn_2S_6] demonstrated an increased sorption capacity with the increase in the concentrations of $[ReO_4]^-$. This experiment led to a maximum rhenium capture capacity (q_m) of 9.8×10^4 and 5.7×10^4 μg/g at pH ~ 2 and 7, respectively, for an initial concentration of 3×10^5 ppb. This value of sorption capacity at pH ~ 2 (9.3×10^4 μg/g) is higher than other materials, namely nano-TiO_2 ~ 71 μg/g,[41] nano-SiO_2 ~ 4.9×10^3 μg/g,[42] polydimethylaminaethyl methacrylate (PolyDMAEMA) hydrogel ~30.5×10^3 μg/g,[43] biochar ~46.5×10^3 μg/g,[32] $Yb_3O(OH)_6Cl$ ~ 48.6×10^3 μg/g,[44] Notre Dame Thorium Borate-1 (NDTB-1) ~ 4.9×10^4 μg/g,[44] nanoscale zero-valent iron supported on reduced graphene oxide (NZVI/rGOs) ~ 8.6×10^4 μg/g,[41] and comparable to resins (PP-g-2-VP) ~ 11.3×10^4 μg/g.[32]

According to a previous report, about 202 mg of nonintercalated Mg/Al-LDH can remove about 8.27×10^{-5} mol/L of perrhenate which is equivalent to 15.4 ppm of Re.[45] Hence, the removal of the ReO_4^- is attributed to anion exchange. In the present study, only 10 mg of LDH-Sn_2S_6 is used which yields the removal of 93 ppm of Re for the equal mass of previously reported LDH. These findings imply that functionalization of LDH by tin sulfides is necessary to achieve high efficiency. Moreover, we also observed the formation of Re containing Sn- and S-based phase. This observation further suggests the necessity of the functionalization of LDH structure with Sn_2S_6 anions for the efficient removal of perrhenate. This finding relevant to LDH functionalization by sulfides or metal sulfides has already been well established earlier for the separation of other metal ions.[17,46,47]

To understand the effects of competitive anions, we analyzed the ReO_4^- removal by LDH-[Sn_2S_6] in a solution containing Cl^-, Br^-, I^-, PO_4^{3-}, SO_4^{2-}, NO_3^-, and CH_3COO^- with a concentration of 1000 ppb of each, at neutral pH. This analysis revealed that ReO_4^- removal is ~35.2% in 24 h, which is lower than the experiments conducted in deionized water for the same concentration and time scale. This finding suggests that LDH-[Sn_2S_6] can remove ReO_4^- from complex solutions, as described above. Wang and Gao[48] developed a correlation between the basal spacing d_{003} of the LDH and the ionic radius and ratio of the M^{II} and M^{III} layered cations. This correlation determines that TcO_4^- sorption efficiency varies with the ionic size of the layered cations and the interlayer distance of LDH. This, along with the diversity of various metal sulfide anions for the intercalation of LDH, suggests that with proper optimization of the chemical compositions, more efficient LDH could be revealed.

After the sorption experiments, the solid samples were analyzed by XRD, SEM, high-resolution TEM (HRTEM), and XPS (Figures 3, 4, S1, and S2). XRD of the ReO_4^- interacted

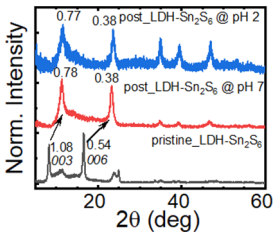

Figure 3. XRD patterns of the pristine and the postinteracted LDH-[Sn_2S_6] with $[ReO_4]^-$ showing the shifting of the *00l* peaks of the LDH structures toward higher two theta value suggesting the decrease in the unit cell along the crystallographic *c*-axis.

LDH-[Sn_2S_6] shows the retention of the LDH structure. Our results show that for both acidic and neutral conditions, the d_{003} peaks, which represent the interplanar distance between the two positively charged layers, decrease from 1.07 to 0.78 nm after the interactions with the ReO_4 anion. Hence, such a decrease of the basal space, d_{003} is related to the shrinkage of the LDH's crystal structure along the *c*-axis. This should be because of the intercalation of the smaller ReO_4 anion by the exchange of the larger Sn_2S_6 ions. Hence, this kind of shrinkage of the crystallographic c axis of the LDH was observed for the ion exchange of the MoS_4 anion of the LDH-MoS_4 with CrO_4^{2-} and SeO_4^{2-}/SeO_3^{2-}.[17,38,40,47−50]

The postinteracted samples were also analyzed by SEM and HRTEM, revealing detailed insight into the morphology and

https://doi.org/10.1021/acsaenm.3c00074
ACS Appl. Eng. Mater. XXXX, XXX, XXX−XXX

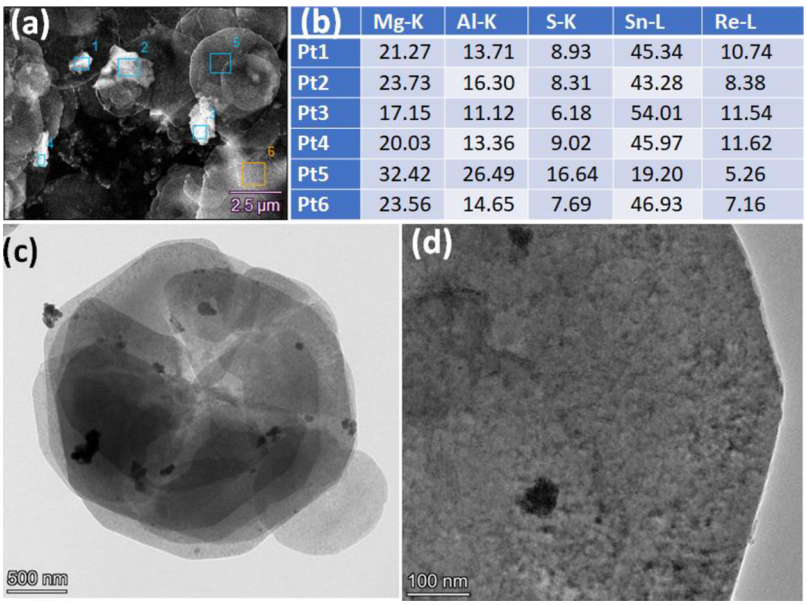

(b)	Mg-K	Al-K	S-K	Sn-L	Re-L
Pt1	21.27	13.71	8.93	45.34	10.74
Pt2	23.73	16.30	8.31	43.28	8.38
Pt3	17.15	11.12	6.18	54.01	11.54
Pt4	20.03	13.36	9.02	45.97	11.62
Pt5	32.42	26.49	16.64	19.20	5.26
Pt6	23.56	14.65	7.69	46.93	7.16

Figure 4. SEM image (a), EDX in weight percentage (b), TEM image at different length scales (c, d) showing the morphology, chemical compositions, and the presence of the second phase in the postinteracted LDH-Sn_2S_6.

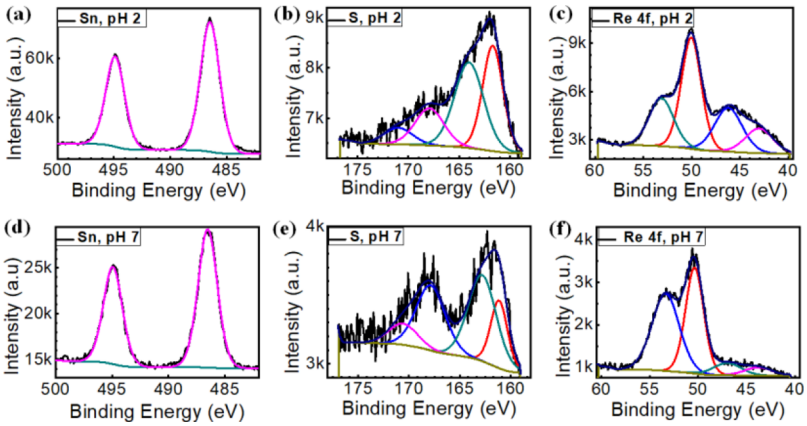

Figure 5. XPS spectra after sorption of 100 ppm ReO_4^- by LDH-$[Sn_2S_6]$ at pH 2 (a–c) and 7 (d–f) showing the presence of Sn, S, and Re as well as their corresponding oxidation states.

chemical compositions (Figures 4, S1, and S2). The experiments show the presence of hexagonal platelike crystallites of LDH along with the formation of irregularly shaped nanoaggregated secondary phase. EDS of both phases shows the presence of rhenium. This suggests that besides ion exchange, precipitation of rhenium contributes to the removal of perrhenate from the solution. Additionally, surface adsorption of oxoanions via hydrogen bonding between the LDH's surface exposed $O-H^{\delta+}$ and oxygen of $[ReO_4]^-$ as LDH-$O-H^{\delta+}-O$-Re is known.[19,35,37] Therefore, one can presume that this phenomenon may present for the LDH-$[Sn_2S_6]$.

We also analyzed LDH-$[Sn_2S_6]$ by X-ray photoelectron spectroscopy after the interactions with $[Re^{7+}O_4]^-$ at pH values ~2 and 7 (Figure 5). These analyses revealed the bands centered at ~486 and ~494 eV, which are attributed to the photoelectron energies of the $3d_{5/2}$ and $3d_{3/2}$ orbitals of Sn, respectively, both in the acidic and neutral mediums. These values of binding energies correspond to the tetravalent oxidation state of tin, Sn^{4+}.[51] This suggests that retention of the IV+ oxidation of Sn as in the $[Sn_2S_6]^{4-}$ ions. Similarly, we observed two bands centered at about 164.0 and 161.6 eV. These are representative of binding energies for the S^{2-} 2p orbitals.[51] In addition, XPS spectra also showed two additional bands centered at ~168.0 and ~171.0 eV, which are attributed to the 2p orbital energies of $S^{4+/6+}$.[52,53] Hence, these values of the binding energies suggest the partial oxidation of sulfide ions to sulfate/sulfites.[52] XPS of the ReO_4^- interacted LDH-$[Sn_2S_6]$ shows the presence of weak peaks at 42.90 and 46.13 eV, which could be originated from the Re 4f orbitals.[54−56] Importantly, the weak peak at about 42.90 eV is attributed to the Re^{4+} oxidation states, while the peak at about 46.12 eV corresponds to the Re^{7+} oxidations.[54−56] Notably, the strong peak at about 50.05 eV could be the superimposed peaks of Re $4f_{5/2}$ and Mg 2p orbital energies.[56] The presence of Re^{7+} in the postinteracted samples may suggest the presence of ReO_4^- ions, which can be attributed to ion exchange, as evidenced by XRD (Figure 3). Additionally, the known phenomenon of surface sorption, as discussed above, may also contribute to the sorption of the ReO_4^- ions.[19,35,37] Besides, the presence of Re^{4+} ions can be understood by the reduction of highly soluble Re^{7+} ($\equiv Re^{7+}O_4^-$) to insoluble/sparingly soluble Re^{4+} species, which could be attributed to reductive precipitation of irregular

https://doi.org/10.1021/acsaenm.3c00074
ACS Appl. Eng. Mater. XXXX, XXX, XXX−XXX

sized and shaped agglomerated particles as we see in the SEM and HRTEM (Figure 4).

Notably, the reduction of $Re^{7+} \rightarrow Re^{4+}$ could be attributed to partial oxidation of S^{2-} of $[Sn_2S_6]^{4-} \rightarrow S^{4+/6+} + ne^-$ (SO_3^{2-}/SO_4^{2-}). The oxidation of S^{2-} of the Sn_2S_6 to SO_3^{2-}/SO_4^{2-} has already been seen in the XPS spectra of the postinteracted samples with the prominent peaks in the region of 168−172 eV (Figure 5b,e). Analogous to the previous report of the reductive precipitation of high valent transition metal cations, such as Cr^{6+}, this finding suggests the reductive precipitation of highly soluble $Re^{7+}O_4^-$ to insoluble Re^{4+} species can be attributed to the oxidation of the sulfides of the Sn_2S_6 anions.[16,19] Hence, the high standard redox potentials of Re^{7+} ($Re^{7+}O_4^-$ is E° ~0.51 V) enables its reduction to Re^{4+} by the sulfide, $S^{2-} \rightarrow S^{n+} + ne^-$ (e.g., E° of S^{2-}/SO_4^{2-} is −0.172 V) of LDH-Sn_2S_6.[57] Hence, oxidation of the sulfides to sulfite/sulfate in an acidic solution is plausibly more prominent. This ultimately also accelerates the removal of ReO_4^- through reductive precipitation.

4. CONCLUSIONS

We showed that LDH-$[Sn_2S_6]$ is an efficient sorbent for ReO_4^-, which is an isoelectronic and structural surrogate of $^{99}TcO_4^-$. This material achieved >98 and 89% removal of rhenium from ppm levels down to ppb in acidic and neutral solutions. The sorption kinetics of ReO_4^- for LDH-$[Sn_2S_6]$ follows the pseudo-second-order rate equations but the sorption mechanisms vary for the acidic and neutral solutions. In addition, we discovered that the presence of 3d transition metal ions, such as Cu^{2+}, greatly increases the efficiency of ReO_4^- removal to almost 100% for a 1000 ppb solution of Re^{7+} in an acidic medium. This results in residual concentrations below 1 ppb and a K_d value of ~5.0×10^7 mL/g. Our research also shows that LDH-$[Sn_2S_6]$ has a high capacity for Re^{7+} removal, with a capacity of about 9.3×10^4 μg/g. The sequestration of ReO_4^- may occur through a cooperative contribution of ion exchange, surface sorption, and reductive precipitation, where the sulfide ion acts as a reductant, converting highly soluble $Re^{7+}O_4^-$ to insoluble Re^{4+} species. This finding differs from the other type of metal sulfide intercalated LDH, e.g., LDH-Mo_3S_{13}, which shows a remarkable efficiency for chromate, as a redox surrogate of pertechnetate, removal from solutions. For the LDH-Mo_3S_{13}, chromate separation is predominantly accomplished by the reduction of soluble Cr(VI) to insoluble Cr(III) species.[16] Hence, such a distinction between the LDH-Mo_3S_{13} and LDH-Sn_2S_6 can be articulated by the presence of the mono and disulfide species of the $[Mo_3S_{13}] \equiv [MoS(S_2)_6]^{2-}$ and the absence of the disulfide (S_2^{2-}) for the $[Sn_2S_6]^{4-}$ ion. Overall, these results suggest that metal sulfide functionalized LDHs are a promising class of sorbents for removing $[^{99}TcO_4]^-$ anions. Despite this fact, due to the complex compositions of the legacy nuclear waste, a comprehensive investigation of chemical compositions, interplanar space, and interlayer anions of LDHs is required to understand the true potential of this class of materials for the separation of $[^{99}TcO_4]^-$ from legacy nuclear wastes.

ASSOCIATED CONTENT

Supporting Information

The Supporting Information is available free of charge at https://pubs.acs.org/doi/10.1021/acsaenm.3c00074.

Kinetic data and parameters for the sorption of ReO_4^- by the LDH-$[Sn_2S_6]$; SEM images and EDS spectra of post sorbed LDH-Sn_2S_6 at pH 2 and 7 (PDF)

AUTHOR INFORMATION

Corresponding Author

Saiful M. Islam − *Department of Chemistry, Physics, and Atmospheric Sciences, Jackson State University, Jackson, Mississippi 39217, United States;* orcid.org/0000-0001-8518-1856; Email: muhammad.s.islam@jsums.edu

Authors

Ahmet Celik − *Department of Chemistry, Physics, and Atmospheric Sciences, Jackson State University, Jackson, Mississippi 39217, United States*

Subrata Chandra Roy − *Department of Chemistry, Physics, and Atmospheric Sciences, Jackson State University, Jackson, Mississippi 39217, United States*

Michael A. Quintero − *Department of Chemistry, Northwestern University, Evanston, Illinois 60208, United States;* orcid.org/0000-0002-0709-1676

Kathryn Taylor-Pashow − *Savannah River National Laboratory, Aiken, South Carolina 29808, United States;* orcid.org/0000-0002-1986-0866

Dien Li − *Savannah River National Laboratory, Aiken, South Carolina 29808, United States*

Mercouri G. Kanatzidis − *Department of Chemistry, Northwestern University, Evanston, Illinois 60208, United States;* orcid.org/0000-0003-2037-4168

Xianchun Zhu − *Department of Civil Engineering, Jackson State University, Jackson, Mississippi 39217, United States*

Complete contact information is available at: https://pubs.acs.org/10.1021/acsaenm.3c00074

Author Contributions

This manuscript was written through the contributions of all authors. All authors have given approval to the final version of the manuscript. A. Celik and S. C. Roy authors have contributed equally to this work.

Notes

The authors declare no competing financial interest.

ACKNOWLEDGMENTS

This work was partially supported by the US Department of Energy Minority Serving Institution Partnership Program (MSIPP) managed by the Battelle Savannah River Alliance, LLC under the BSRA contract (RFP No. 0000542525 and 00004583570). SCR is thankful to the NSF Division of Chemistry (NSF-2100797). This also was supported in part by the Department of Energy's Nuclear Energy University Program (NEUP) through project 21-24188 (M.G.K.). All the ICP-MS analyses were conducted at JSU's core research centers supported by RCMI (NIH grant: 1U54MD015929). This work made use of the Keck-II facility of Northwestern University's NUANCE Center, which has received support from the SHyNE Resource (NSF ECCS-2025633), the IIN, and Northwestern's MRSEC program (NSF DMR-1720139). TEM images were taken in part at the Chapel Hill Analytical and Nanofabrication Laboratory, CHANL, a member of the North Carolina Research Triangle Nanotechnology Network, RTNN, which is supported by the National Science

Foundation, Grant ECCS-2025064, as part of the National Nanotechnology Coordinated Infrastructure, NNCI.

REFERENCES

(1) Xiao, C.; Khayambashi, A.; Wang, S. Separation and Remediation of $^{99}TcO_4^-$ from Aqueous Solutions. *Chem. Mater.* **2019**, *31*, 3863−3877.

(2) Lee, M.-S.; Um, W.; Wang, G.; Kruger, A. A.; Lukens, W. W.; Rousseau, R.; Glezakou, V.-A. Impeding ^{99}Tc(IV) Mobility in Novel Waste Forms. *Nat. Commun.* **2016**, *7*, 12067.

(3) Dickson, J. O.; Harsh, J. B.; Flury, M.; Lukens, W. W.; Pierce, E. M. Competitive Incorporation of Perrhenate and Nitrate into Sodalite. *Environ. Sci. Technol.* **2014**, *48*, 12851−12857.

(4) Li, J.; Chen, L.; Shen, N.; Xie, R.; Sheridan, M. V.; Chen, X.; Sheng, D.; Zhang, D.; Chai, Z.; Wang, S. Rational Design of a Cationic Polymer Network towards Record High Uptake of $^{99}TcO_4^-$ in Nuclear Waste. *Sci. China Chem.* **2021**, *64*, 1251−1260.

(5) Li, J.; Li, B.; Shen, N.; Chen, L.; Guo, Q.; Chen, L.; He, L.; Dai, X.; Chai, Z.; Wang, S. Task-Specific Tailored Cationic Polymeric Network with High Base-Resistance for Unprecedented $^{99}TcO_4^-$ Cleanup from Alkaline Nuclear Waste. *ACS Cent. Sci.* **2021**, *7*, 1441−1450.

(6) Mei, L.; Li, F.; Lan, J.; Wang, C.; Xu, C.; Deng, H.; Wu, Q.; Hu, K.; Wang, L.; Chai, Z.; Chen, J.; Gibson, J. K.; Shi, W. Anion-Adaptive Crystalline Cationic Material for $^{99}TcO_4^-$ Trapping. *Nat. Commun.* **2019**, *10*, 1532.

(7) DiPrete, D. P.; DiPrete, C. C.; Sigg, R. A. Measurement of ^{99}Tc in Savannah River Site High Activity Waste. *J. Radioanal. Nucl. Chem.* **2005**, *263*, 593−598.

(8) King, W. D.; Hassan, N. M.; McCabe, D. J.; Hamm, L. L.; Johnson, M. E. Technetium Removal from Hanford and Savannah River Site Actual Tank Waste Supernates with Superlig®639 Resin. *Sep. Sci. Technol.* **2003**, *38*, 3093−3114.

(9) Banerjee, D.; Kim, D.; Schweiger, M. J.; Kruger, A. A.; Thallapally, P. K. Removal of TcO_4^- Ions from Solution: Materials and Future Outlook. *Chem. Soc. Rev.* **2016**, *45*, 2724−2739.

(10) Eagling, J.; Worsfold, P. J.; Blake, W. H.; Keith-Roach, M. J. Mobilization of Technetium from Reduced Sediments under Seawater Inundation and Intrusion Scenarios. *Environ. Sci. Technol.* **2012**, *46*, 11798−11803.

(11) Shen, N.; Yang, Z.; Liu, S.; Dai, X.; Xiao, C.; Taylor-Pashow, K.; Li, D.; Yang, C.; Li, J.; Zhang, Y.; Zhang, M.; Zhou, R.; Chai, Z.; Wang, S. $^{99}TcO_4^-$ Removal from Legacy Defense Nuclear Waste by an Alkaline-Stable 2D Cationic Metal Organic Framework. *Nat. Commun.* **2020**, *11*, 5571.

(12) Li, J.; Dai, X.; Zhu, L.; Xu, C.; Zhang, D.; Silver, M. A.; Li, P.; Chen, L.; Li, Y.; Zuo, D.; Zhang, H.; Xiao, C.; Chen, J.; Diwu, J.; Farha, O. K.; Albrecht-Schmitt, T. E.; Chai, Z.; Wang, S. $^{99}TcO_4^-$ Remediation by a Cationic Polymeric Network. *Nat. Commun.* **2018**, *9*, 3007.

(13) Sheng, D.; Zhu, L.; Xu, C.; Xiao, C.; Wang, Y.; Wang, Y.; Chen, L.; Diwu, J.; Chen, J.; Chai, Z.; Albrecht-Schmitt, T. E.; Wang, S. Efficient and Selective Uptake of TcO_4^- by a Cationic Metal−Organic Framework Material with Open Ag^+ Sites. *Environ. Sci. Technol.* **2017**, *51*, 3471−3479.

(14) El Mouzdahir, Y.; Elmchaouri, A.; Mahboub, R.; ElAnssari, A.; Gil, A.; Korili, S. A.; Vicente, M. A. Interaction of Stevensite with Cd^{2+} and Pb^{2+} in Aqueous Dispersions. *Appl. Clay Sci.* **2007**, *35*, 47−58.

(15) Ma, L.; Wang, Q.; Islam, S. M.; Liu, Y.; Ma, S.; Kanatzidis, M. G. Highly Selective and Efficient Removal of Heavy Metals by Layered Double Hydroxide Intercalated with the MoS_4^{2-} Ion. *J. Am. Chem. Soc.* **2016**, *138*, 2858−2866.

(16) Celik, A.; Li, D.; Quintero, M. A.; Taylor-Pashow, K. M. L.; Zhu, X.; Shakouri, M.; Roy, S. C.; Kanatzidis, M. G.; Arslan, Z.; Blanton, A.; Nie, J.; Ma, S.; Han, F. X.; Islam, S. M. Removal of CrO_4^{2-}, a Nonradioactive Surrogate of $^{99}TcO_4^-$, Using LDH−Mo_3S_{13} Nanosheets. *Environ. Sci. Technol.* **2022**, *56*, 8590−8598.

(17) Roy, S. C.; Rahman, M. A.; Celik, A.; Wilson, S.; Azmy, A.; Bieber, J.; Spanopoulos, I.; Islam, R.; Zhu, X.; Han, F. X.; Islam, S. M. Efficient Removal of Chromium(VI) Ions by Hexagonal Nanosheets of CoAl-MoS_4 Layered Double Hydroxide. *J. Coord. Chem.* **2022**, *75*, 1581−1595.

(18) Yang, L.; Xie, L.; Chu, M.; Wang, H.; Yuan, M.; Yu, Z.; Wang, C.; Yao, H.; Islam, S. M.; Shi, K.; Yan, D.; Ma, S.; Kanatzidis, M. G. $Mo_3S_{13}^{2-}$ Intercalated Layered Double Hydroxide: Highly Selective Removal of Heavy Metals and Simultaneous Reduction of Ag^+ Ions to Metallic Ag^0 Ribbons. *Angew. Chem., Int. Ed.* **2022**, *61*, No. e202112511.

(19) Pearce, C. I.; Moore, R. C.; Morad, J. W.; Asmussen, R. M.; Chatterjee, S.; Lawter, A. R.; Levitskaia, T. G.; Neeway, J. J.; Qafoku, N. P.; Rigali, M. J.; Saslow, S. A.; Szecsody, J. E.; Thallapally, P. K.; Wang, G.; Freedman, V. L. Technetium Immobilization by Materials through Sorption and Redox-Driven Processes: A Literature Review. *Sci. Total Environ.* **2020**, *716*, 132849.

(20) Neeway, J. J.; Asmussen, R. M.; Lawter, A. R.; Bowden, M. E.; Lukens, W. W.; Sarma, D.; Riley, B. J.; Kanatzidis, M. G.; Qafoku, N. P. Removal of TcO_4^- from Representative Nuclear Waste Streams with Layered Potassium Metal Sulfide Materials. *Chem. Mater.* **2016**, *28*, 3976−3983.

(21) Fan, D.; Anitori, R. P.; Tebo, B. M.; Tratnyek, P. G.; Lezama Pacheco, J. S.; Kukkadapu, R. K.; Engelhard, M. H.; Bowden, M. E.; Kovarik, L.; Arey, B. W. Reductive Sequestration of Pertechnetate ($^{99}TcO_4^-$) by Nano Zerovalent Iron (NZVI) Transformed by Abiotic Sulfide. *Environ. Sci. Technol.* **2013**, *47*, 5302−5310.

(22) Ma, S.; Chen, Q.; Li, H.; Wang, P.; Islam, S. M.; Gu, Q.; Yang, X.; Kanatzidis, M. G. Highly Selective and Efficient Heavy Metal Capture with Polysulfide Intercalated Layered Double Hydroxides. *J. Mater. Chem. A* **2014**, *2*, 10280−10289.

(23) Müller, A.; Bhattacharyya, R. G.; Pfefferkorn, B. Eine Einfache Darstellung Der Binären Metall-Schwefel-Cluster $[Mo_3S_{13}]^{2-}$ Und $[Mo_2S_{12}]^{2-}$ Aus MoO_4^{2-} in Praktisch Quantitativer Ausbeute. *Chem. Ber.* **1979**, *112*, 778−780.

(24) Celik, A.; Baker, D. R.; Arslan, Z.; Zhu, X.; Blanton, A.; Nie, J.; Yang, S.; Ma, S.; Han, F. X.; Islam, S. M. Highly Efficient, Rapid, and Concurrent Removal of Toxic Heavy Metals by the Novel 2D Hybrid LDH−$[Sn_2S_6]$. *Chem. Eng. J.* **2021**, *426*, No. 131696.

(25) Kanatzidis, M.; Riley, B.; Chun, J.; Sarma, D.; Kota, S. S.; Pierce, D. A. *Novel Metal Sulfides to Achieve Effective Capture and Durable Consolidation of Radionuclides; P.N. 12-3438*; 2016; pp 1−32.

(26) Sarma, D.; Islam, S. M.; Subrahmanyam, K. S.; Kanatzidis, M. G. Efficient and Selective Heavy Metal Sequestration from Water by Using Layered Sulfide $K_{2x}Sn_{4-x}S_{8-x}$ (x = 0.65−1; KTS-3). *J. Mater. Chem. A* **2016**, *4*, 16597−16605.

(27) Westsik, J. H.; Cantrell, K. J.; Serne, R. J.; Qafoku, N. Technetium Immobilization Forms Literature Survey; PNNL-23329, EMSP-RPT-023; 2014; pp 1−64.

(28) Liu, T.; Yang, M.; Wang, T.; Yuan, Q. Prediction Strategy of Adsorption Equilibrium Time Based on Equilibrium and Kinetic Results To Isolate Taxifolin. *Ind. Eng. Chem. Res.* **2012**, *51*, 454−463.

(29) Azizian, S. Kinetic Models of Sorption: A Theoretical Analysis. *J. Colloid Interface Sci.* **2004**, *276*, 47−52.

(30) *Handbook of Layered Materials*; Auerbach, S. M.; Carrado, K. A.; Dutta, P. K., Eds.; CRC Press: Boca Raton, 2019.

(31) Goh, K.-H.; Lim, T.-T.; Dong, Z. Application of Layered Double Hydroxides for Removal of Oxyanions: A Review. *Water Res.* **2008**, *42*, 1343−1368.

(32) Zu, J. H.; Wei, Y. Z.; Ye, M. S.; Tang, F. D.; He, L. F.; Liu, R. Q. Preparation of a New Anion Exchanger by Pre-Irradiation Grafting Technique and Its Adsorptive Removal of Rhenium(VII) as Analogue to 99Tc. *Nucl. Sci. Technol., 26*, 69−75, DOI: 10.13538/j.1001-8042/nst.26.S10302.

(33) Lieser, K. H.; Bauscher, C. Technetium in the Hydrosphere and in the Geosphere: II. Influence of PH, of Complexing Agents and of Some Minerals on the Sorption of Technetium. *Radiochim. Acta* **1988**, *44*−*45*, 125−128.

https://doi.org/10.1021/acsaenm.3c00074
ACS Appl. Eng. Mater. XXXX, XXX, XXX−XXX

(34) Lieser, K. H.; Bauscher, C. Technetium in the Hydrosphere and in the Geosphere: Technetium in the Hydrosphere and in the Geosphere. *Radiochim. Acta* **1987**, *42*, 205−214.
(35) Johnston, A.-L.; Lester, E.; Williams, O.; Gomes, R. L. Understanding Layered Double Hydroxide Properties as Sorbent Materials for Removing Organic Pollutants from Environmental Waters. *J. Environ. Chem. Eng.* **2021**, *9*, No. 105197.
(36) Daniels, N.; Franzen, C.; Murphy, G. L.; Kvashnina, K.; Petrov, V.; Torapava, N.; Bukaemskiy, A.; Kowalski, P.; Si, H.; Ji, Y.; Hölzer, A.; Walther, C. Application of Layered Double Hydroxides for ^{99}Tc Remediation. *Appl. Clay Sci.* **2019**, *176*, 1−10.
(37) Chao, Y.-F.; Lee, J.-J.; Wang, S.-L. Preferential Adsorption of 2,4-Dichlorophenoxyacetate from Associated Binary-Solute Aqueous Systems by Mg/Al-NO_3 Layered Double Hydroxides with Different Nitrate Orientations. *J. Hazard. Mater.* **2009**, *165*, 846−852.
(38) Tanaka, K.; Kozai, N.; Yamasaki, S.; Ohnuki, T.; Kaplan, D. I.; Grambow, B. Adsorption Mechanism of ReO_4^- on Ni−Zn Layered Hydroxide Salt and Its Application to Removal of ReO_4^- as a Surrogate of TcO_4^-. *Appl. Clay Sci.* **2019**, *182*, No. 105282.
(39) Tanaka, K.; Kozai, N.; Ohnuki, T.; Grambow, B. Study on Coordination Structure of Re Adsorbed on Mg−Al Layered Double Hydroxide Using X-Ray Absorption Fine Structure. *J. Porous Mater.* **2019**, *26*, 505−511.
(40) Ma, L.; Islam, S. M.; Xiao, C.; Zhao, J.; Liu, H.; Yuan, M.; Sun, G.; Li, H.; Ma, S.; Kanatzidis, M. G. Rapid Simultaneous Removal of Toxic Anions $[HSeO_3]^-$, $[SeO_3]^{2-}$, and $[SeO_4]^{2-}$, and Metals Hg^{2+}, Cu^{2+}, and Cd^{2+} by MoS_4^{2-} Intercalated Layered Double Hydroxide. *J. Am. Chem. Soc.* **2017**, *139*, 12745−12757.
(41) Li, J.; Chen, C.; Zhang, R.; Wang, X. Reductive Immobilization of Re(VII) by Graphene Modified Nanoscale Zero-Valent Iron Particles Using a Plasma Technique. *Sci. China Chem.* **2016**, *59*, 150−158.
(42) Li, Y.; Wang, Q.; Li, Q.; Zhang, Z.; Zhang, L.; Liu, X. Simultaneous Speciation of Inorganic Rhenium and Molybdenum in the Industrial Wastewater by Amino-Functionalized Nano-SiO_2. *J. Taiwan Inst. Chem. Eng.* **2015**, *55*, 126−132.
(43) Yan, Y.; Yi, M.; Zhai, M.; Ha, H.; Luo, Z.; Xiang, X. Adsorption of ReO_4^- Ions into PolyDMAEMA Hydrogels Prepared by UV-Induced Polymerization. *React. Funct. Polym.* **2004**, *59*, 149−154.
(44) Zhu, L.; Xiao, C.; Dai, X.; Li, J.; Gui, D.; Sheng, D.; Chen, L.; Zhou, R.; Chai, Z.; Albrecht-Schmitt, T. E.; Wang, S. Exceptional Perrhenate/Pertechnetate Uptake and Subsequent Immobilization by a Low-Dimensional Cationic Coordination Polymer: Overcoming the Hofmeister Bias Selectivity. *Environ. Sci. Technol. Lett.* **2017**, *4*, 316−322.
(45) Kang, M. J.; Rhee, S. W.; Moon, H. Sorption of MO_4^- (M = Tc, Re) on Mg/Al Layered Double Hydroxide by Anion Exchange. *Radiochim. Acta* **1996**, *75*, 169−174.
(46) Bai, P.; Dong, Z.; Wang, S.; Wang, X.; Li, Y.; Wang, Y.; Ma, Y.; Yan, W.; Zou, X.; Yu, J. A Layered Cationic Aluminum Oxyhydroxide as a Highly Efficient and Selective Trap for Heavy Metal Oxyanions. *Angew. Chem., Int. Ed.* **2020**, *59*, 19539−19544.
(47) Rathore, E.; Maji, K.; Biswas, K. Nature-Inspired Coral-like Layered $[Co_{0.79}Al_{0.21}(OH)_2(CO_3)_{0.11}]\cdot mH_2O$ for Fast Selective Ppb Level Capture of Cr(VI) from Contaminated Water. *Inorg. Chem.* **2021**, *60*, 10056−10063.
(48) Wang, Y.; Gao, H. Compositional and Structural Control on Anion Sorption Capability of Layered Double Hydroxides (LDHs). *J. Colloid Interface Sci.* **2006**, *301*, 19−26.
(49) Kang, M. J.; Chun, K. S.; Rhee, S. W.; Do, Y. Comparison of Sorption Behavior of I^- and TcO^-_4 on Mg/Al Layered Double Hydroxide. *Radiochim. Acta* **1999**, *85*, 57−64.
(50) Mahmoud, M. R.; Someda, H. H. Mg−Al Layered Double Hydroxide Intercalated with Sodium Lauryl Sulfate as a Sorbent for $^{152+154}$Eu from Aqueous Solutions. *J. Radioanal. Nucl. Chem.* **2012**, *292*, 1391−1400.
(51) Li, R.; Jiang, K.; Chen, S.; Lou, Z.; Huang, T.; Chen, D.; Shen, G. SnO_2/SnS_2 Nanotubes for Flexible Room-Temperature NH_3 Gas Sensors. *RSC Adv.* **2017**, *7*, 52503−52509.
(52) Powell, C. *X-Ray Photoelectron Spectroscopy Database XPS, Version 4.1, NIST Standard Reference Database 20*; 1989.
(53) X-ray Photoelectron Spectroscopy (XPS) Reference Pages. http://www.xpsfitting.com/search/label/Sulphur (accessed December 2022).
(54) Crist, B. V. Rhenium Spectra - Re Native Oxide. The International XPS Database 1. https://xpsdatabase.com/rhenium-spectra-re-native-oxide/ (accessed December 2022).
(55) Crist, B. V. XPS in Industry—Problems with Binding Energies in Journals and Binding Energy Databases. *J. Electron Spectrosc. Relat. Phenom.* **2019**, *231*, 75−87.
(56) *Handbook of X-Ray Photoelectron Spectroscopy: A Reference Book of Standard Spectra for Identification and Interpretation of XPS Data, Update*; Moulder, J. F.; Chastain, J., Eds.; Perkin-Elmer Corporation: Eden Prairie, MI, 1992.
(57) Key, J.; David, B. *Introductory Chemistry-1st Canadian Edition*, 1st edition; Pressbooks by BCcampus, Chapter: Appendix, 2014.

https://doi.org/10.1021/acsaenm.3c00074
ACS Appl. Eng. Mater. XXXX, XXX, XXX−XXX